

Experimental and FEM Characterization of Rayon Fibre

Johnson Ezenwankwo*, Iva Petrikova and Josef Zak

Department of Applied Mechanics, Technical University of Liberec, Liberec, Czech Republic

Abstract

Natural and synthetic fibre has gained wide application in science and technology. They are now used as reinforcement material for composites in automobile, aviation, textile, apparel and other related industries. In spite of their inherent drawbacks (disposal method, anisotropic nature, production cost and technical complexities) natural fibres present a wide range of advantages ranging from availability, eco-friendliness and a reasonable competitiveness with sheet metals and other counterparts. Natural fibres, in particular, offer light weight as well as good strength when used both as a reinforcement material in various matrix configurations. In this article, the behaviour and response of samples of a 4-ply viscose rayon material loaded in tension is investigated. The response of viscose-rayon yarn in various tensile loading configurations was carried out. Two types of single fibre multifilament material is cut out from separate spools 1840 dtex and 2440 dtex; the remaining two samples tested were plain woven fabric – single and 4-layer. These tensile tests were done to estimate the maximum yield strength of the material and the onset of plastic behaviour. A Unit Cell (UC) of the material is developed in TexGen, commercial software, as a Representative Volume Element (RVE). The model is imported into an FEA tool and the simulation results are compared. Symmetry and periodic boundary conditions are imposed using the planar symmetry function in Ansys and the simple Dirichlet boundary condition in terms of displacement. The results showed good agreement with the experimental results and helped to characterize the material for further use in composite development.

Keywords: Unit Cell (UC) • Response • Rayon • Characterization

Introduction

In recent times, material science and technology has experienced a huge shift in paradigm motivated by the global idea of environmental protection and the need to replace non-bio-degradable materials with naturally biodegradable alternatives [1]. From 2017, the global demand for carbon fibre has soared to about 70.5 k tons for 114.7 k tons of Carbon-Fibre-Reinforced Plastics (CFRP). CFRP is used for various engineering applications ranging from high temperature automobile parts, machine parts under fatigue load and other parts where the use of metals could prove more expensive [2]. Another major concern is the issue of waste where up to 30% of the material involved in the manufacturing process is discarded as waste mainly in form of scrap with little or no prospect of reuse or recycle [3]. The need to switch to bio-degradable, renewable and environmentally-friendly materials has presented natural fibres as a viable alternative as intermediate and reinforcement materials for composites. Low density and cost-effectiveness are reported as two of the main features that make natural fibres popular in automotive and construction industries, Ramesh M, et al. [4] and Bajaj P, et al. [5] recorded such desirable properties as absence of static problems, ability to resist peeling associated with surface degradation and abrasion, great dyeing characteristics for aesthetics, low or slow rate of wear, tear and obsolescence, relatively good compatibility with other fibres and a remarkable wear property. In all fairness, there are also pre-existing demerits and challenges associated with the use of natural fibres; the most notable of these being lack of durability - especially when sisal fibre was used as an intermediate reinforcement material for concrete composites [6]. Other challenges involve high water absorption (hydrophilic properties) which has been shown to have adverse effects on the tensile strength of viscose

rayon. Based on this, Ramesh M, et al. [7] tested the impact of water uptake in Banana-Carbon hybrid fibre reinforced polymer composite as it affects its mechanical properties. They concluded that water uptake increased with the introduction of natural fibre as a hybrid with carbon fibre and vital mechanical properties experienced a significant drop. Low impact strength and low thermal properties are also other concerns when natural fibre reinforced composites are employed in automobile car bodies where impact absorption plays a major role in events of high-impact collision. In spite of these challenges, natural fibre remains one of the choicest types of reinforcement material. Studies have shown the durability of concrete slabs reinforced with sisal fibre and submitted that sisal fibre contributed significantly in improving the mechanical properties of the concrete-sisal fibre. Tagarielli VL, et al. [8] addressed the issue of an efficient and reliable method to measure the through-thickness of a material owing to the sheer difficulty in manufacturing thick laminates with relatively high thickness. The study also recapped that the onset of failure as it occurs in through-thickness cases in composites laminates largely depend on direct and shear inter-laminar stresses. Paul SA, et al. [9] used banana-leaves composites in a tensile test and also monitored the effect of chemical alteration on the composites. The study showed the role of chemical treatment and how it improves the thermo-physical properties of the material tested. Weave architecture greatly affects the response of fibre to multiaxial, in-plane and out-of-plane pure shear loading. Kaw AK [10] presented an in-depth study of fibre (natural/synthetic) reinforced composites – in his book, he expounded the concept of failure of composites, several damage models including Tsai-Wu, Tsai-Hill, Hoffmann and others were explored.

Boominathan SK, et al. [11] carried out an investigation of a special fibre called *A. Concinna* used as a reinforcement agent for polyester resin. The study looked at the effect of fibre length, fibre weight percentage. The composite was tested for moisture absorption and tensile strength and impact toughness for both the raw and the treated samples. It has also been known that chemical treatment greatly affects the mechanical property of materials by favourably altering the crystalline pattern of such materials through interstitials when molecules fit themselves in gaps created by the arrangement of the main molecules. A specialized method of a thermal analyzer was used to obtain the mass degradation pattern when the physical, chemical, thermal and surface morphological properties of bark fibre extracts from *A. Concinna* were studied by Venugopal A and Senthil KB [12]. The research analyzed the suitability of the fibre as reinforcement member in composite systems by varying the chemical composition of the treatment agent and monitoring how it affects the cellulose and hemicellulose in the fibre. A thermo-gravimetric analysis

*Address for Correspondence: Johnson Ezenwankwo, Department of Applied Mechanics, Technical University of Liberec, Liberec, Czech Republic; E-mail: johnson.ezenwankwo@tul.cz

Copyright: © 2024 Ezenwankwo J, et al. This is an open-access article distributed under the terms of the Creative Commons Attribution License, which permits unrestricted use, distribution, and reproduction in any medium, provided the original author and source are credited.

Received: 16 February, 2024, Manuscript No. jtese-24-127746; Editor Assigned: 19 February, 2024, PreQC No. P-127746; Reviewed: 04 March, 2024, QC No. Q-127746; Revised: 09 March, 2024, Manuscript No. R-127746; Published: 18 March, 2024, DOI: 10.37421/2165-8064.2024.14.585

was carried out to determine the thermal stability and maximum degradation temperature. Weave architecture and fibre orientation play great role in the mechanical response of woven and non-woven preforms.

Amutha V and Senthilkumar B [13] and Ivars J, et al. [14] used recycled carbon fibre materials as reinforcement materials as a way to combat soil pollution while aiming to curb problems of disposal of these materials after their useful life – Ivars studied the fibre orientation and distribution on the mechanical behaviour of the samples used. The study evaluated the tensile, bending and performing response of the preform and also the influence of the stacking order of multi-layer layout on its compression response. The hydrophilic tendency of natural fibre, as mentioned earlier, is a phenomenon of great concern in textile technology and dynamics. Most research works have found that wet fabrics loss up to 50% of their mechanical properties.

Abd El-Baky MA and Kamel M [15] studied the abrasive wear behaviour of jute-glass-carbon –reinforced composites by comparing stacking sequence and relative fibre amounts. In the study, nine different laminates were produced by hand lay-up method and the specimens were soaked in water for up to 60 days. The results revealed the marked improvement in abrasive wear resistance of the material. This article further showed that fibre relative volume has more effect on wear resistance than the stacking sequence. D'Anna J, et al. [16] investigated the mechanical properties of basalt fibre as a reinforcement element in Fibre-Reinforced Matrix Composite (FRCM). The work analyzed the effect of such properties as geometrics, clamping system of test set up (especially considering slippage, measurement system and test speed (rate) all on the evaluation of the tensile properties of basalt fibre. A study with similar material, fibre reinforced cementitious composite but with kenaf fibre, was carried out by Abbas AGN, et al. [17]. The results expounded on the need for more use of natural fibre in place of their synthetic counterpart. Furthermore it investigated the flexural and tensile properties of the fibre considering such properties as fibre length and fibre percentage content.

The use of finite element tools has proven to predict the behaviour of materials to a highly reasonable accuracy and agreement. Finite element modelling through specialized software have brought on user-friendly and easy but accurate means to model the geometry needed for textile geometrics modelling and simulation [18]. There is a number of commercial software to help engineers and scientists to represent the actual behaviour of their model as input for analysis. Wang Y, et al. [19], Drach B, et al. [20] and Nilakantan G, et al. [21] used various methods to create unit cells and RVEs models for performing simulations to analyze the behaviour of fabrics of different weaving mechanics and architectures.

Erol O, et al. [22] studied the effect of weave architecture on the mechanical properties of woven fabric. Plain, twill, basket and satin weave configurations were generated as unit cells and analyzed. The study also captured the effect of transverse shear modulus of the yarns while also studying such relations as shear angle as it affects the normalized frictional energy and unit torque. Drach A, et al. [23] investigated the processing of chosen architecture during finite element modelling of 3D woven composites. The work further described the problem of discontinuity in geometry along the path of the fibre due to effect of tensile and contact pressure as is captured in the so-called “nominal geometry”. The multi-chain digital element method was proposed by Wang Y and Sun X [24]. The idea is that each fibre is represented as a digital rod-like element. This study seeks to experimentally determine the key mechanical properties of viscose-rayon yarn tested in three different forms, a fabric sheet, a single yarn (1840 dtex from spool and a 2440 dtex from fabric) and a 4-ply fabric stack. The fibre strength, Young's modulus as well as total displacement of several uniaxial tests were recorded and plotted. A unit cell of the fibre was generated and analyzed in FEA to draw a comparison of the results obtained.

Materials

The materials are woven at the Textile Faculty of the Technical University of Liberec. The thickness of the woven material is measured using standard method (ASTM D1777-96). A prescribed weight of 100 g is placed between two plates of known thicknesses containing the fabric. The thickness of the

whole setup is measured using a vernier caliper with 0.001 accuracy. The thicknesses of both plates are then subtracted from the overall thickness of plates and fabric. This required especially when modelling the UC in Texgen. To account for experimental and systemic errors, several samples are tested and the average values recorded. During the experiment, the stoppage criterion was set such that when the value of force is has dropped 50% of the highest value or when there is substantial visible rupture and breakage [25-27].

Methodology

The experiment begins with laying out the viscose-rayon fabric and measuring out the samples to be cut. The fabric is a simple-woven fabric with the following geometric properties: thickness 0.388 mm, yarn spacing 0.7 mm (gap between adjacent yarns) and yarn width 0.6 mm (the distance measure from the end of one yarn to the same end of the next yarn). As specified by standards (ASTM) (Zwick/Roell), two dark markings were made on the sides of the specimens facing the light of the extensometer; the rayon-yarn has a golden contrasting colour which enhances a high-contrast transition at the specimen vertical edges. At both ends of the specimen, dark markings which appeared as black lines were selected as targets using the video-extensometer software which automatically photo-detects these zones. The level diagram coloured black resulting from the contrasting background in image was already set to capture high sharpness at the dark zones which form the target edges [28].

Plain fabric fineness test

This test specifically shows the strength of the woven fabric in its original woven form. It helps to characterize the material for properties such as elastic behaviour, yield stress leading up to plastic deformation and finally the softening zone that initiated the break or rupture. The experimental setup involved a specialized clamp manufactured in the fabrication workshop at the Technical University of Liberec. As shown in Figure 1, the crosshead measures 260 mm in length and has an inbuilt studded zone up to 30 mm of its trapezoidal height. The clamps are specially manufactured to suit this particular test. The pins are dispersed all over the locking latch to cover most of the surface that make up the clamping zone on both sides. The 1 mm-diameter pin-like studs provide a seemingly node-to-node grip which digs into the yarn spacing while the latch presses the yarn network down flat onto the clamp ensuring a supreme hold.

Tensile strength test setup

The setup is as shown in Figure 2. The dimension of the fabric is 250 mm × 250 mm. The specimen is clamped on both sides of the support via the spikes of 1 mm diameter and locked with the latch and screw-washer system. The strain rate is preset at 1 mm/min so that an ample number of data points are captured during the uniaxial loading. This helps to better represent and show the full behaviour and response of the material as loading progresses. The gauge length is given as 190 mm. To account for the effect of machine and other instrument errors, 10 samples were tested to more reliable capture the true behaviour of the plain fabric.

Four-ply woven fabric

The second set of specimens involved cutting out a new sample with a dimension of 210 × 240 mm and folded in the weft (transverse) direction to make 4-ply sheet so that there are 4 vertical parallel plies of 210 × 60 mm. Sample gauge length was set at 105 mm (clamping 52.5 mm on both sides to ensure a no-slip tight grip). Five other samples measuring 250 mm × 250 mm were cut out and folded in the same configuration as the first one. Yarn thickness which was fed into TexGen to develop the unit cell was measured



Figure 1. Clamp head for fabric tensile test.

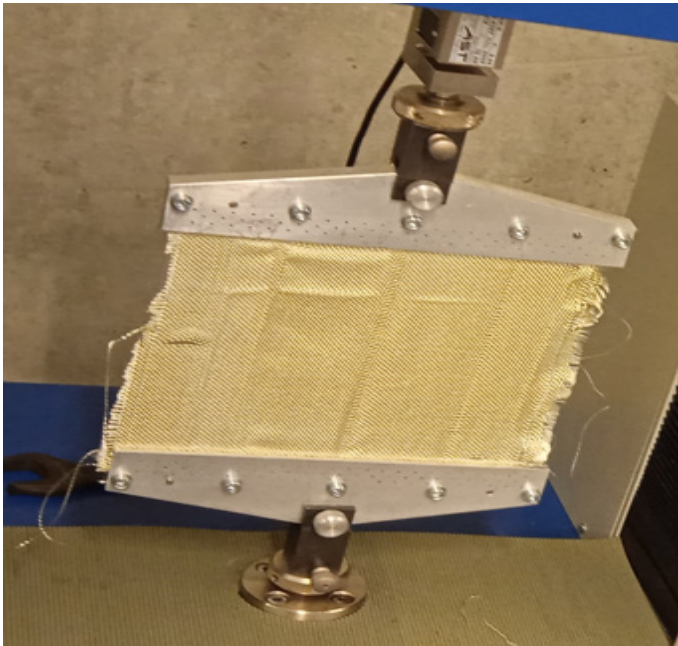


Figure 2. Experimental setup in fineness test.

using a simplified means where two plates of known thickness are mounted on a stand. One notable method for thickness measurement was presented by (Mahmoudi and Oxenham). The rate of displacement was set at 1 mm/min for all tests cases. The sample is loaded until visible breakage is reached or the load reaches drops to 50% of its highest value. This is set automatically on the tensile testing machine. Figure 3 below shows the experimental set up of the 4-ply test. The uni-axial test is mounted on tensile testing machine of up to 30 kN capacity. The inside part of the clamp is serrated to improve fabric hold [29].

Single yarn in tension

The third set up was single yarn testing in tension. Two types of single yarns were tested. The first being a 1840 dtex yarn from a spool and a 2440 dtex single yarn drawn out from a plain-woven fabric - these taxonomy is gotten from the material data sheet of the manufacturers. An initial sample measuring 108 cm was cut from the 1840 dtex spool and the weight was measured. The sample weighed 0.2732 g. The weighing machine is a high-sensitivity weighing device with 0.1 mg accuracy and equipped with a glass enclosure to cut out the environmental effect of draught. This was used later to calculate key parameters of the 1840 dtex spool yarn. The setup consists of winding the yarn specimen around a horizontal spindle covered with leather to improve grip and friction to ensure a strong a hold during tensioning. The rate of loading was 1 mm/minute until the yarn practically snaps after the softening zone. Figure 4 above shows the laboratory setup. A total of 21 samples each of the 1840 dtex spool and the 2440 dtex were tested. A gauge length of 180 mm was used. The repeated winding completely eliminates any chance of slippage during loading. This test was performed on the Tira T280 multiteesting apparatus.

FEM simulation

The simulation was performed in ANSYS and Marc-Mentat. As pointed out in the Introduction, the UC is modelled in TexGen and exported as a standalone step file. A prescribed displacement of 0.5 mm is applied on one side of the UC (two faces on this same side). The opposite side of this is constrained in all direction to form an encastre boundary condition [30]. The other remaining two sides are constrained to move only in the same direction as the tensile load to satisfy for uniaxial loading. If an axi-symmetric model is developed, the model is constrained in the direction perpendicular to the plane(s) of symmetry. Contacts between yarns are setup differently for Ansys and Marc-Mentat: in Ansys, the contact are automatically inserted by reason of proximity with inbuilt tolerance of a few millimeters. In Marc-Mentat, the each yarn is created as a contact body; contact interactions are created and assigned through a contact table. Contact behaviour can present a somewhat complex situation in applied mechanics and greatly affects the global behaviour of the

bodies involved. Both in tensile and compressive zones during burst, rupture, frictional sliding of touching bodies or glued (bonded) bodies with the freedom to slide as is seen in yarn-yarn interaction in the UC. Coulomb's friction rule is famous for stick-slip behaviour on contact interaction zones Hirmand M, et al. [31]. Return mapping algorithm was used to impose the frictional contact implemented by the augmented Lagrangian framework. The complexity and difficulty of modelling contact interaction in finite element practices is the fact that boundaries in contact tend to break into indeterminate directions from their originally defined, undamaged state. A deeper understanding of the idea of contact interaction is captured in the works of Belytschko T, et al. [32], Simo JC and Laursen [33] and Wriggers P [34]. The simulation, just like the experiment, will present 3 cases for the fabric tensile test modelled as a unit cell, the 4-ply experiment modelled as a 4-layer unit cell and the single yarn experiment (from spool and woven-drawn) modelled as one of the four member yarns of the UC. The results are discussed in sequence in the next section. To reduce computation time, it is always a good practice in FEA to employ symmetry where the model is halved (1/2) or quartered (1/4); thus, leaving only a portion of the full model which representatively captures the behaviour of the complete model. The material specifications for the UC are given in Table 1 below. (Figure 5)

Experimental data fit

In Marc-mentat, the experimental data fit is performed by importing the stress-strain test data obtained from the force-displacement data collected from the tensile testing machine. A number of plasticity flow stress models including: Power Law, Modified Power Law, Johnson-Cook, GMT0-2 Models

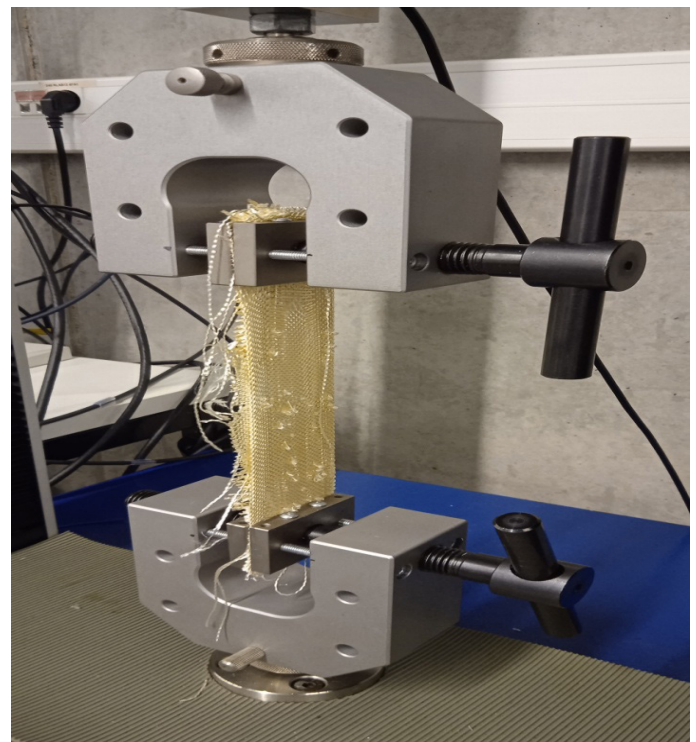


Figure 3. Test machine setup during loading.

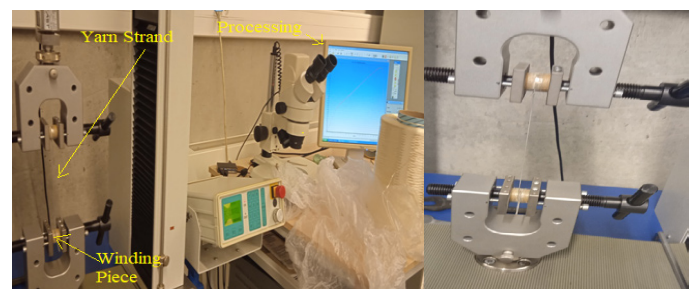


Figure 4. One strand of 1840 dtex in a universal tensile testing setup.

Table 1. Specification of viscose-rayon yarn.

Fibre Density	Fibre Modulus (GPa)	Yarn Linear Density	Areal Density	Poisson Ratio	Fabric Thickness	Yarn Width	Yarn Spacing	Yarn Cross-sectional Area (mm ²)
(kg/m ³)		(g/km)	(kg/m ²)			(mm)		
2560	7	220	310	0.35	0.388	0.6	0.7	0.08493

and Hockett-Sherby Model were tried in application using material data fit in Marc. The best model fit as seen from Figure 6 is the (Glass-Mat-Reinforced Thermoplastic Composite (GMT-1). This is because it showed the best fit along the plot of the experimental data inputted. The discontinuities and noise along the path of the experimental data plot could be explained as filament ruptures within the yarns, at early stage and also outright yarn breakage as seen in the later stages of the plot. The experimental data fit is done using the best data obtained from the experiment in Section 3 as a generalized behaviour of the viscose-rayon yarn material.

Results and Discussion

This section describes the results of the various force-displacement plots and a comparison of the various plots. The cross-sectional area of the yarn is obtained from the UC model in Ansys after inputting the material specifications measured and inserted during the creation of the UC model in TexGen. The plots are mainly of the same material under the same condition so that the research seeks to show the effect of machine on testing various samples under unifying conditions.

Testing the single layer plain woven fabric

This section describes the result of testing the monolayer woven fabric. The setup is shown earlier in Figure 2 with the single-layer fabric. Figure 7 below shows the plots of force and displacement for 5 different specimens tested. The average value is used to develop the stress-strain plot.

Four-ply fabric test

The result of the 4-ply fabric test is described in Figure 8b below. As was expected, the maximum force at the onset of fibre cracking was 7.5 kN, about 98% more than the maximum force needed to initiate fibre cracking in the single-ply test in Section 3.4. The region with the thick lines captures the area of instability as individual fibres began to snap. The zone of thin line shows the onset of the fracture on the very first filament at 5.9 kN at a displacement of 10.33 mm whereas the areas marked with thick lines indicates regions of sustained filamentary failure before the loading was terminated. Figure 8a below shows a combined plot of five other samples folded into 4-ply and tested at ideally the same condition. The graph shows a continuous but noisy increment in displacement as force was increased. Of the five samples tested, one sample reached a maximum force of 5.8 kN before it witnessed considerable fibre damage. The lowest recorded maximum force was 4.7 kN which is 18.97% less than the highest maximum force recorded.

As can be seen from Figures 8 above, there was no preload and the data was set to record the force-displacement relation from origin (0, 0). The result for the third batch of tests, in this section with a preload of 300 N is shown in Figure 9. In Figure 10, tests of 4 samples are shown. A second plot of the same data details where the modified displacement was gotten from zeroing the displacement at the onset and repeating the plot as shown below. The average displacement at significant damage is 15 mm after which filament ruptures causing the tensile force to drop. No problem was recorded with grips at the clamps; so no significant slip was experienced.

Single fibre test

As describes in Section 3.4, single yarn filaments were loaded in tension on a tensile testing machine. The crosshead speed was same as other experiments until outright rupture occurred. The data collected was used to calculate the average modulus of the material. First, the standard Hookean relation is used to calculate the yarn stiffness as read off from Figure 11 above.

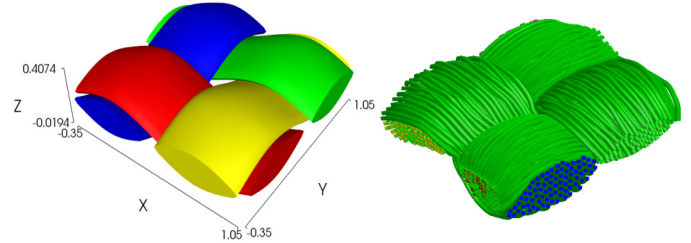


Figure 5. Simple weave unit cell model a) TexGen (mesoscale) and b) DFCA (81-fibre microscale).

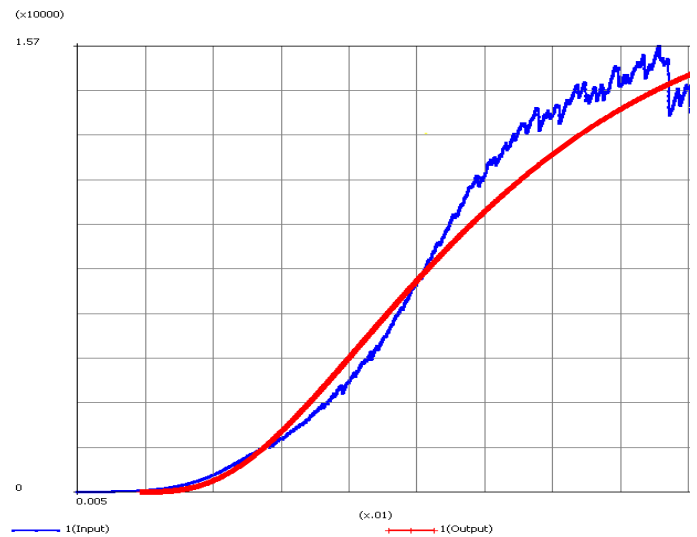


Figure 6. Experimental data (blue ragged) vs. GMT-1 plasticity flow stress model.

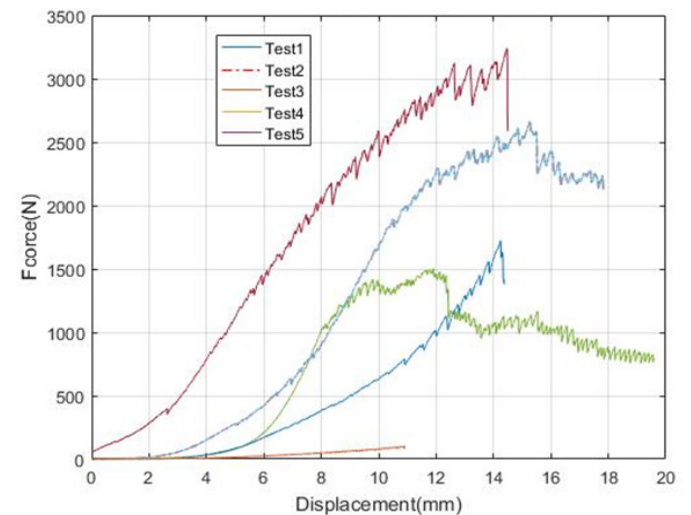


Figure 7. Plot of single-ply test.

FEM output

As shown in Figure 12 below, there are 4 contact zones with 318 faces on each side of the interacting domains. In Ansys, the contact faces are detected automatically by reason of proximity. In Marc-Mentat, 4 meshed-deformable bodies are created and 4 glued-type self-contact interactions are applied each

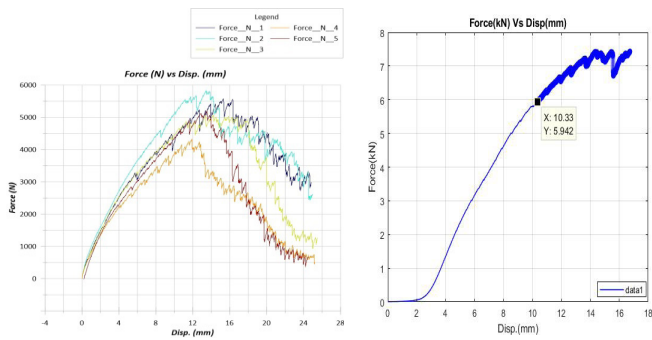


Figure 8. a) Force-displacement (210 × 240 mm 4-ply) and b) force-displacement plot (250 × 250 mm 4-ply).

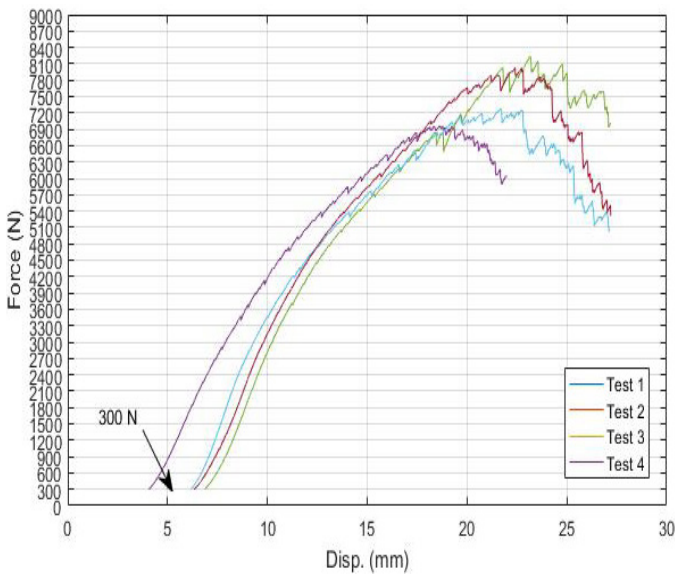


Figure 9. Preload samples test plots.

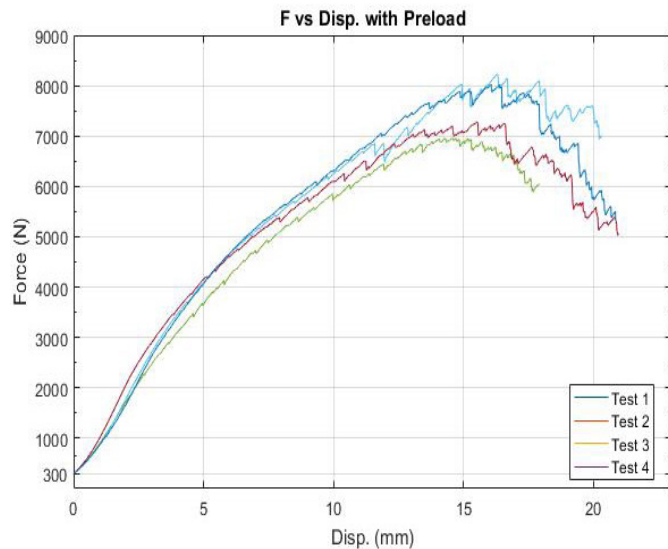


Figure 10. 300-N preloaded test plots with modified displacement values.

neighbouring pairs of yarn through the contact table. Failure was mostly due to transverse shear at the contact zones, fibre reactive forces. The filament interactions are ignored since the model is developed at mesoscale. From History Plot function, path plot, nodal plots and global plots are generated. The model, as shown in Figure 12, has 4 contact zones with 318 faces apiece in target-contact interaction as captured in Ansys static structural analysis. The rest of the simulation is completed in Mar-Mentat. The plots and simulation results are described. Figure 13 below shows the contour plot of

the displacement in the x-direction where the prescribed displacement was applied. The deformed and the wireframe profile of the original shape with the regions around the load application showing the highest displacement and the contact force being highest around the 4 contact zones mentioned earlier.

The contact ensures the glued-to-touching relationship between yarn to yarn is maintained and that horizontal fibres are drawn in the x-axis only and that the vertical fibres move laterally being constrained in the y and z directions while ignoring the effect of fibre crimps. The strain energy-time plot is shown as a path plot choosing the nodes along a specified path-in this case two instances were of emphasis, a path along the x-axis and a second one along the y-axis. The plot is shown in Figure 14 below and depicts the total of all energies from bending, compression and tension at elemental level in the UC during the application load. The plot of distance and displacement in the x-11 direction of displacement is seen in Figure 14b. Six set of nodes on the face of prescribed displacement was used for the plot. The maximum von Mises stress is given as 1.056 GPa. The equivalent stress is plotted against the equivalent elastic strain in Figure 15a with a maximum value of 1.571 GPa for the equivalent of stress and the shear stress with a maximum value of 2.098 GPa is captured in Figure 15b with the same set of nodes as in Figure 15a.

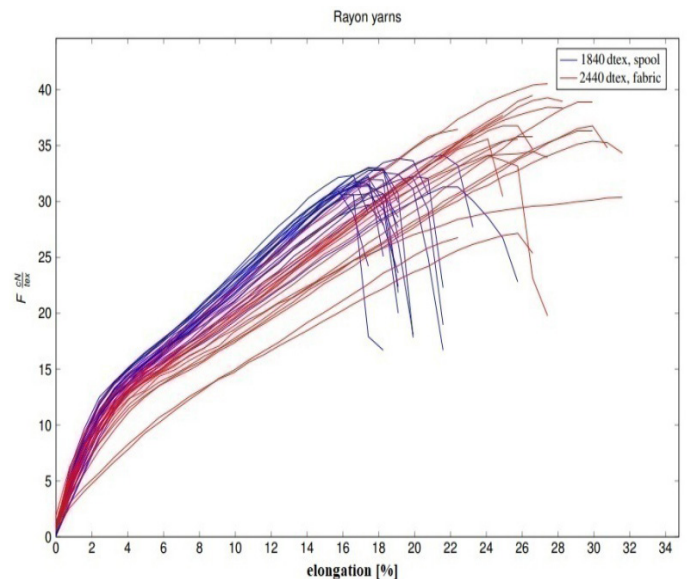


Figure 11. Woven and spool (unwoven) fibre test plots.

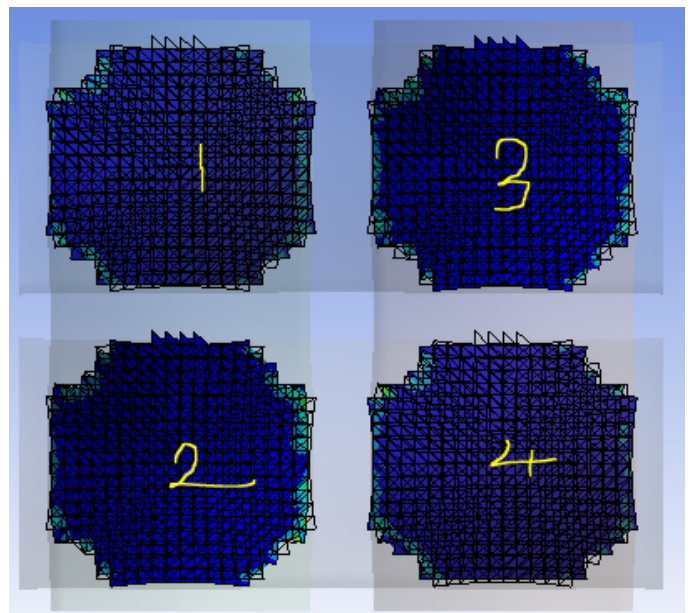


Figure 12. Contact zones of the UC in ansys.

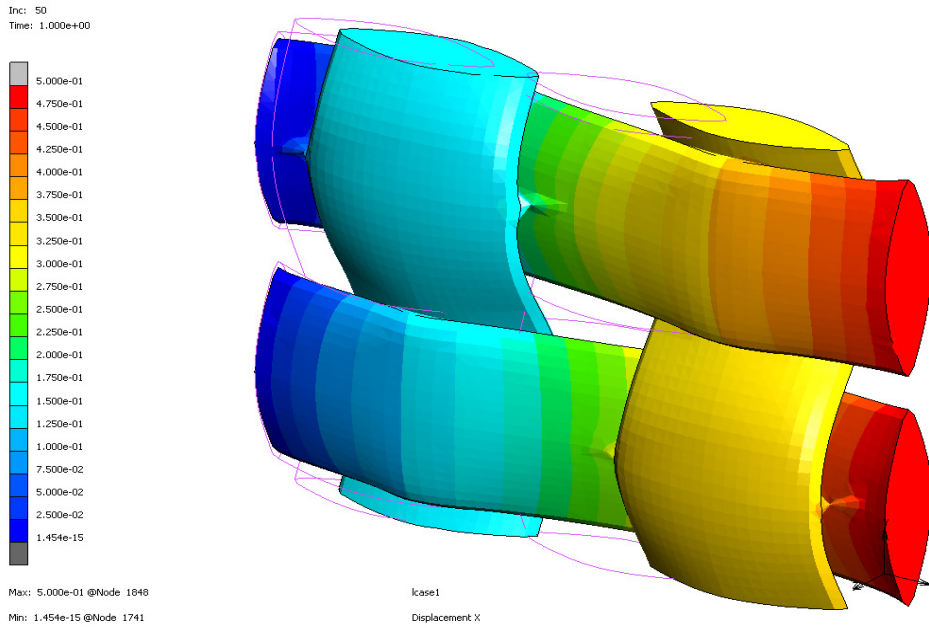


Figure 13. Contour plot of x-displacement (deformed and outline of original shape).

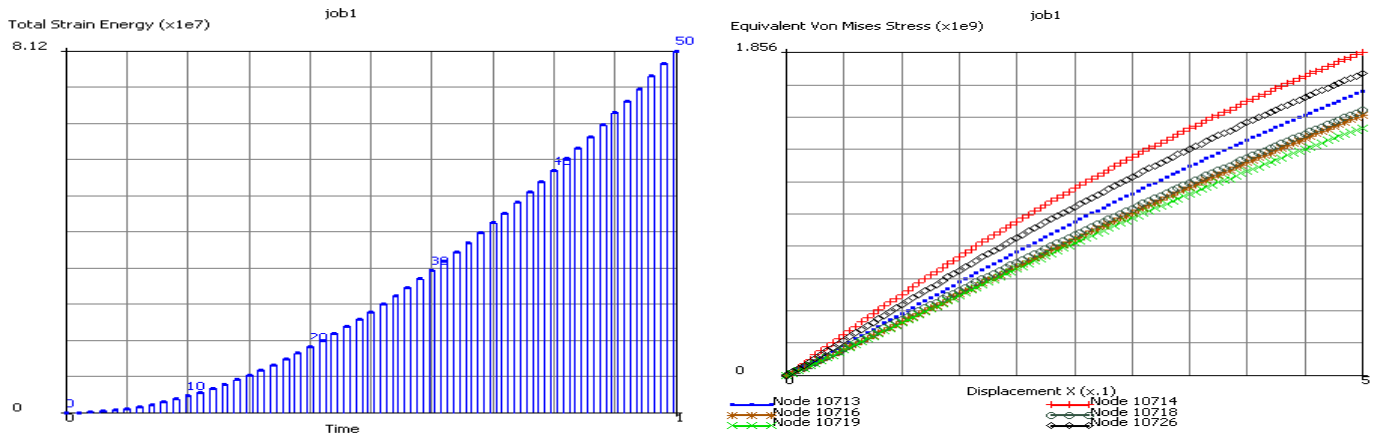


Figure 14. a) Total strain energy plot and b) Nodal equivalent von mises stress and displacement.

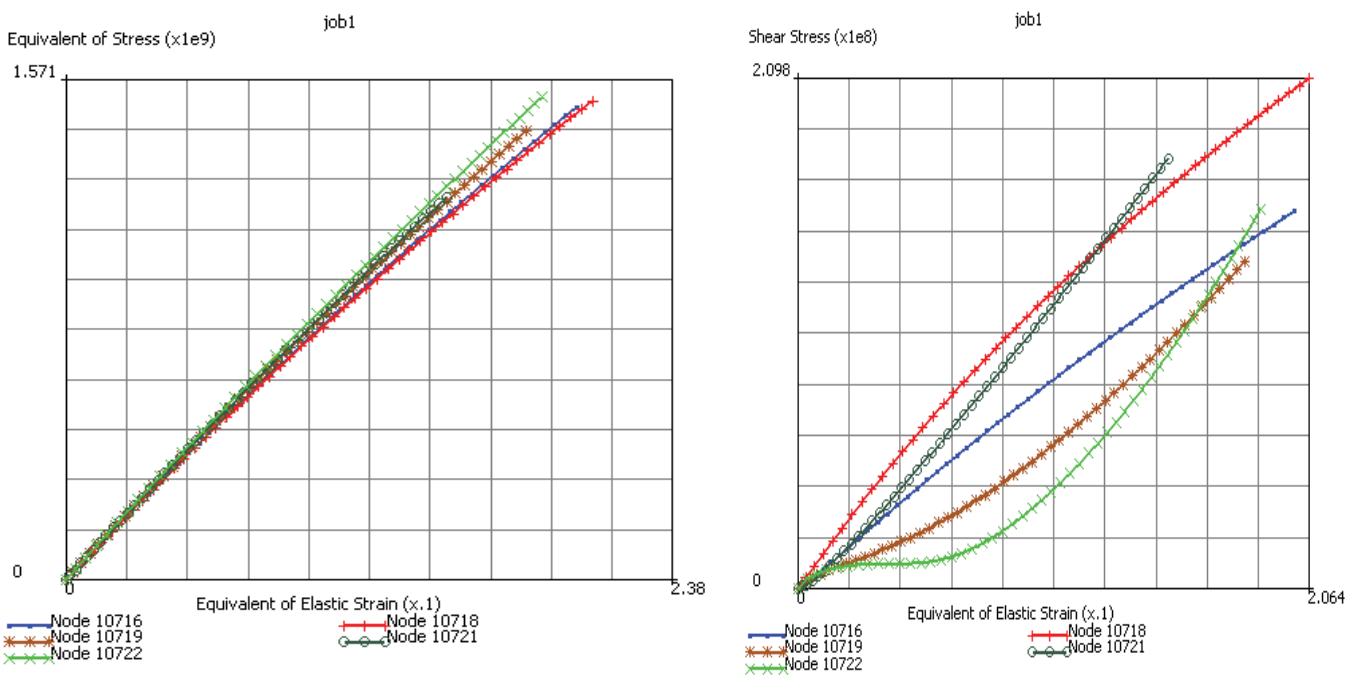


Figure 15. a) Eqv. stress vs. eqv. strain and b) Nodal equivalent von mises stress and displacement.

These nodes are areas of high emphasis – especially contact regions between two fibres and the frontal nodes.

Conclusion

The work has shown the capabilities of FEM in modelling the real-life behaviour of an RVE to a reasonable agreement. Apart from these, the materials samples showed similar and recognizable behaviour and response in tension. The FEM model is developed using Marc-Mentat based on the ASTM D527 uni-axial tensile test. The in-built GMT-1 constitutive model based on flow stress best captured the stress-strain experimental data curve under constant loading on the tensile testing machine. The most gainful advantage of employing the FEM is that it easily, but technically, captures the original behaviour of the material under the type of loading in question. The type of behaviour type of frictional interaction at the contact zones was found to greatly affect the response of the RVE in loading. For instance, by adding four symmetry planes in Ansys on the opposing symmetric sides of each of the yarns that make up the RVE, the result showed a more plastic behaviour in the vertical yarn near the load application region, although no separation of interaction zone occurred and the yarns were not able to translate horizontally without having to bend around the mid section. The modelling is found to be greatly dependent on the geometric properties of the model imported for the analysis, including the yarn cross-sectional area of the yarn, yarn topology and shape, loading conditions, type of boundary conditions and constraints and yarn parameters. The plastic hardening model adopted also plays a key role during material definition. The software Comsol Multiphysics also presents a number of isotropic plasticity hardening models including Hockett-Sherby, Voce and Ludwi. In Ansys, the Chaboche nonlinear kinematic hardening model was provided for inputting the stress-strain values which is solved using the curve-fit application and uploaded in the material properties. Marc-Mentat in plasticity flow stress use the power law, the GMTs model and the Hockett-Sherby etc. One of the challenges of the experimental approach is the instrumental error, as such, the test is conducted with several samples and an average (mean) value is adopted with calculation of the standard deviation. The experimental data which had noise in the plot showed good agreement with the GMT1 model. Since the simulation was done considering one plasticity model, further work could be based on comparing the effect of adopting other plasticity model and observing how they affect the response of the chosen RVE. To diversify further, this could also be employed in composite materials RVEs with woven fabric reinforcement and the more popular unidirectional RVE in micromechanics.

Role of Authors

Research Conceptualization and Ideation (E.J., J.Z.); Data Collection and Experiment (E.J., J.Z.); Supervisory Role and Guidance (I.P., J.Z.); Result Interpretation and Analysis (E.J., J.Z.); Writing the Original Draft (E.J.); Review and Comments (I.P., J.Z.).

Funding Statement

This publication was written at the Technical University of Liberec as part of the project "Research of advanced materials and application of machine learning in the area of control and modeling of mechanical systems" nr. SGS-2022-5072 with the support of the Specific University Research Grant, as provided by the Ministry of Education, Youth and Sports of the Czech Republic in the year 2023.

Acknowledgement

None.

Conflict of Interest

The author declares that there is/are no conflict(s) of interest.

References

- Ago, Hiroki, Susumu Okada, Yasumitsu Miyata and Kazunari Matsuda et al. "Science of 2.5 dimensional materials: Paradigm shift of materials science toward future social innovation." *Sci Technol Adv Mater* 23 (2022): 275-299.
- Sauer, Michael and M. Kuhnel. "Composites market report 2019." *Carbon Composites* (2019): 1-11.
- Snudden, J. P., C. Ward and K. Potter. "Reusing automotive composites production waste." *Reinforced Plastics* 58 (2014): 20-27.
- Ramesh, M., T. Sri Ananda Atreya, U. S. Aswin and H. Eashwar et al. "Processing and mechanical property evaluation of banana fiber reinforced polymer composites." *Procedia Eng* 97 (2014): 563-572.
- Bajaj, P., A. K. Sengupta, T. K. Dhar and J. S. Chakraborty, "Texturing viscose rayon." *Indian J Text Res* 4 (1979): 85-90.
- Ravi, K. H., S. Pradeepa, J. Arpit and Ashish, et al. "A study on durability of sisal fibre reinforced concrete composites." *Int J Emerg Technol Adv Eng* 7 (2008).
- Ramesh, Manickam, Ravi Logesh, Manivannan Manikandan and Nithyanandam Sathesh Kumar et al. "Mechanical and water intake properties of banana-carbon hybrid fiber reinforced polymer composites." *Mater Res* 20 (2017): 365-376.
- Tagarielli, V. L., G. Minisgallo, A. J. McMillan and N. Petrinic. "The response of a multi-directional composite laminate to through-thickness loading." *Compos Sci Technol* 70 (2010): 1950-1957.
- Paul, Sherey Annie, Abderrahim Boudenne, Laurent Ibos and Yves Candau et al. "Effect of fiber loading and chemical treatments on thermophysical properties of banana fiber/polypropylene commingled composite materials." *Compos - A: Appl Sci Manuf* 39 (2008): 1582-1588.
- Kaw, Autar K. "Mechanics of composite materials." CRC Press 2005.
- Boominathan, Senthil Kumar, V. Amutha, P. Senthamaraiannan and D. Vijay Kirubhakar Raj et al. "Investigation of mechanical, thermal and moisture diffusion behavior of *A. Concinna* fiber/polyester matrix composite." *J Nat Fibers* 19 (2022): 13495-13510.
- Venugopal, Amutha and Senthil Kumar Boominathan. "Physico-chemical, thermal and tensile properties of alkali-treated acacia concinna fiber." *J Nat Fibers* 19 (2022): 3093-3108.
- Amutha, V. and B. Senthilkumar. "Physical, chemical, thermal and surface morphological properties of the bark fiber extracted from *A. Concinna* plant." *J Nat Fibers* 18 (2021): 1661-1674.
- Ivars, Jean, Ahmad Rashed Labanieh and Damien Soulat. "Effect of the fibre orientation distribution on the mechanical and preforming behaviour of nonwoven preform made of recycled carbon fibres." *Fibers* 9 (2021): 82.
- Abd El-Baky, M. A. and M. Kamel. "Abrasive wear performance of jute-glass-carbon-reinforced composites: Effect of stacking sequence and fibers relative amounts." *J Nat Fibers* (2019).
- D'Anna, Jennifer, Giuseppina Amato, Jianfei Chen and Giovanni Minafò et al. "Effects of different test setups on the experimental tensile behaviour of basalt fibre bidirectional grids for FRCM composites." *Fibers* 8 (2020): 68.
- Abbas, Al-Ghazali Noor, Farah Nora Aznieta Abdul Aziz, Khalina Abdan and Noor Azline Mohd Nasir et al. "Kenaf fibre reinforced cementitious composites." *Fibers* 10 (2022): 3.
- Lin, Hua, Louise P. Brown and Andrew C. Long. "Modelling and simulating textile structures using TexGen." *Adv Mater Res* 331 (2011): 44-47.
- Wang, Youqi, Agniprobho Mazumder, Binghui Liu and Chian-Fong Yen. "Applications of digital element approach in textile mechanics and textile composite mechanics." In *Proceedings of the American Society for Composites, Thirty-fifth Technical Conference* (2020).
- Drach, B., A. Drach, I. Tsukrov and M. Penverne et al. "Finite element models of 3D woven composites based on numerically generated micro-geometry of reinforcement." In *Proceedings of the American Society for Composites 2014-29th Technical Conference on Composite Materials* (2014).
- Nilakantan, Gaurav, Michael Keefe, Travis A. Bogetti and Rob Adkinson et al. "On the finite element analysis of woven fabric impact using multiscale modeling techniques." *Int J Solids Struct* 47 (2010): 2300-2315.

22. Erol, Ozan, Brian M. Powers and Michael Keefe. "Effects of weave architecture and mesoscale material properties on the macroscale mechanical response of advanced woven fabrics." *Compos A: Appl Sci Manuf* 101 (2017): 554-566.
23. Drach, Andrew, Borys Drach and Igor Tsukrov. "Processing of fiber architecture data for finite element modeling of 3D woven composites." *Adv Eng Softw* 72 (2014): 18-27.
24. Wang, Youqi and Xuekun Sun. "Digital-element simulation of textile processes." *Compos Sci Technol* 61 (2001): 311-319.
25. Editors, Time-Life (1991). *Inventive Genius*. New York: Time-Life Books. p. 52. ISBN 0-8094-7699-1.
26. Articles on Natural Fibre: <https://www.fibersource.com/f-tutor/rayon.html>
27. Gohl, E. and L. Vilensky. "Sundry facts about Yarns - Textiles for modern living." Melbourne: Longman Cheshire Publ (1990): 190-191.
28. ASTM 2018. Standard test method for ignition loss of cured reinforced resins; ASTM D2584-18;
29. D'Anna, Jennifer, Giuseppina Amato, Jianfei Chen and Giovanni Minafò et al. "Effects of different test setups on the experimental tensile behaviour of basalt fibre bidirectional grids for FRCC composites." *Fibers* 8 (2020): 68.
30. Mahmoudi, M. R. and W. Oxenham. "A new electro-mechanical method for measuring yarn thickness." *Autex Res J* 2 (2002): 28-37.
31. Hirmand, M., M. Vahab and A. R. Khoei. "An augmented Lagrangian contact formulation for frictional discontinuities with the extended finite element method." *Finite Elem Anal Des* 107 (2015): 28-43.
32. Belytschko, Ted, Wing Kam Liu, Brian Moran and Khalil Elkhodary. *Nonlinear finite elements for continua and structures*. John Wiley & Sons (2014).
33. Simo, J. Ci and TA1143885 Laursen. "An augmented lagrangian treatment of contact problems involving friction." *Comput Struct* 42 (1992): 97-116.
34. Wriggers, Peter. "Computational contact mechanics." *Comput Mech* 32 (2003): 141-141.

How to cite this article: Ezenwankwo, Johnson, Iva Petrikova and Josef Zak. "Experimental and FEM Characterization of Rayon Fibre." *J Textile Sci Eng* 14 (2024): 585.